CHIN. PHYS. LETT. Vol. 38, No. 1 (2021) 010503

Isotropic Thermal Cloaks with Thermal Manipulation Function

Quan-Wen Hou(侯泉文)*, Jia-Chi Li(李嘉驰), and Xiao-Peng Zhao(赵晓鹏)

Smart Materials Laboratory, School of Physical Science and Technology, Northwestern Polytechnical University, Xi'an 710129, China

(Received 22 September 2020; accepted 24 November 2020; published online 6 January 2021)

By extending the conventional scattering canceling theory, we propose a new design method for thermal cloaks based on isotropic materials. When the objects are covered by the designed cloaks, they will not disturb the temperature profile in the background zone. In addition, if different inhomogeneity coefficients are selected in the thermal cloak design process, these cloaks can manipulate the temperature gradient of the objects, i.e., make the temperature gradients higher, lower, or equal to the thermal gradient in the background zone. Therefore, thermal transparency, heat concentration or heat shield effects can be realized under a unified framework.

DOI: 10.1088/0256-307X/38/1/010503

Since the pioneering work on introducing the concept of metamaterials to the thermal transfer regime in 2008,[1] research into thermal metamaterials has been developed greatly. Many novel thermal devices based on thermal metamaterials have been proposed, designed, and fabricated to manipulate thermal energy flux, such as thermal cloaks,[2–5] heat flux concentrators,[6,7] a transient thermal shield,[8] heat flux reversers,[3,9,10] a uniform plate heater,[11] macroscopic thermal diodes,[12] illusion thermal devices,[13,14] a remote cooling thermal lens,[15] an encrypted thermal printing device,[16] and temperature-responsive thermal metamaterials.[17]

Of these devices, thermal cloaks, which can eliminate the temperature perturbations caused by objects embedded in the background, have been most extensively investigated. Thermal cloaks are often designed using the coordinate transformation method, in which proper transformations are required to obtain the thermal properties of the cloaks. In most cases, this method leads to anisotropic (inhomogeneous,[4] or homogeneous[18,19]) thermal properties in the cloaks. These characteristics make these cloaks challenging to fabricate.

Another method often applied for designing thermal cloaks is the scattering canceling method,[20,21] based on effective media theory. By coupling objects and cloaks, this method makes the effective properties of the composite (composed of objects and cloaks) the same as those of the background. In this way, the temperature profile of the background will not be disturbed by embedded objects. Compared with the coordinate transformation method, cloaks designed by this method often have isotropic properties. Unfortunately, however, these cloaks can only cloak the object from the background, and cannot manipulate the temperature profile of objects.

Thermal manipulations are important for some applications, such as thermal sensors,[22] energy harvesting,[23] thermal shielding,[24] etc. Thermal cloaks with manipulation functions would therefore have broad appeal in relation to the above applications. Recently, Huang *et al.*[25] proposed a method for the design of multilayer/gradient thermal cloaks. While maintaining the cloaking effect in background, these cloaks were able to realize thermal transparency, heat concentration or heat shielding for the objects. However, similarly to cloaks designed via the coordinate transformation method, these cloaks still require anisotropic properties.

An interesting question therefore arises, as to whether isotropic cloaks can be designed to achieve a cloaking effect and the thermal manipulation of objects simultaneously. The answer is yes. In this work, we propose a method of designing thermal cloaks based on isotropic materials. While thermally cloaking objects from the background, these cloaks can manipulate the thermal fields of objects by means of selecting different inhomogeneities in the cloak. This method is verified experimentally and via simulations.

Let us consider two-dimensional steady heat conduction in a square zone. The schematic structure of such a system is shown in Fig. 1. The left and right boundaries are at high temperature T_1, and low temperature T_2, respectively. The top and bottom boundaries are adiabatic. Next, a circular object (I) with radius r_1 is embedded in the center of the background zone (Ⅲ). Since it possesses different thermal conductivity from the background material, it will disturb the temperature distribution in the background. To

Supported by the National Natural Science Foundation of China (Grant No. 51406168).
*Corresponding author. Email: hqw1983@nwpu.edu.cn
© 2021 Chinese Physical Society and IOP Publishing Ltd

eliminate this disturbance, an annular thermal cloak (Ⅱ), with outer radius r_2, can be used to cover the object. When the thermal conductivity of the cloak is designed properly, the temperature profile outside the cloak will be recovered.

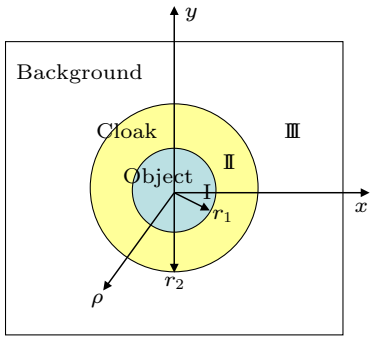

Fig. 1. Schematic of the thermal cloak. Zone I is the object, zone Ⅱ is the cloak, and zone Ⅲ is the background.

The steady heat conduction equations for the object and the background zone are

$$\frac{\partial^2 T_i}{\partial \rho^2}+\frac{1}{\rho}\frac{\partial T_i}{\partial \rho}+\frac{1}{\rho^2}\frac{\partial^2 T_i}{\partial \theta^2}=0,\ (i=\mathrm{I}\ \text{or}\ \mathrm{Ⅲ}). \tag{1}$$

When the cloaking effect is achieved, the temperature distributions of the background and the object are, respectively,

$$T_{\mathrm{Ⅲ}}=a_3\rho\cos\theta+T_{\mathrm{O}}, \tag{2}$$

and

$$T_{\mathrm{I}}=a_1\rho\cos\theta+T_{\mathrm{O}}, \tag{3}$$

where a_3 is the temperature gradient for the background, as determined by the boundary conditions of the system, and T_{O} is the reference temperature in the center of the system. The parameter a_1 is the temperature gradient for the object, which is related to the design of the thermal cloak.

In contrast to thermal cloaks with anisotropic thermal conductivities,[4,19,26] an isotropic and inhomogeneous cloak is considered in this work. Due to the symmetry of the system, the thermal conductivity of the cloak is assumed to be angle-independent, i.e., $\kappa_{\mathrm{c}}=\kappa_{\mathrm{c}}(\rho)$. Hence, the governing equation in cloak zone (Ⅱ) is expressed as

$$\frac{\partial^2 T_{\mathrm{Ⅱ}}}{\partial \rho^2}+\left(\frac{1}{\rho}+\frac{1}{\kappa_{\mathrm{c}}}\frac{d\kappa_{\mathrm{c}}}{d\rho}\right)\frac{\partial T_{\mathrm{Ⅱ}}}{\partial \rho}+\frac{1}{\rho^2}\frac{\partial^2 T_{\mathrm{Ⅱ}}}{\partial \theta^2}=0. \tag{4}$$

The cloaking effect can be realized by cloaks with varying inhomogeneity. For simplicity, we assume that the thermal conductivity of the cloak, κ_{c}, varies exponentially with radius, i.e.,

$$\kappa_{\mathrm{c}}=\beta(\rho/r_1)^{\alpha}, \tag{5}$$

where β is a coefficient related to the magnitude of thermal conductivity, and α is a coefficient related to the inhomogeneity. If $\alpha=0$, the thermal cloak will possess homogenous thermal conductivity.

Solving Eqs. (4) and (5), we can obtain the temperature distribution in cloak zone:

$$T_{\mathrm{Ⅱ}}=\left(b_2\rho^{\frac{-\alpha+\sqrt{\alpha^2+4}}{2}}+c_2\rho^{\frac{-\alpha-\sqrt{\alpha^2+4}}{2}}\right)\cos\theta, \tag{6}$$

where b_2 and c_2 are undetermined coefficients.

Equations (2), (3), and (6) express the temperature profiles in different zones. At the interfaces between the zones, temperature and heatflux continuity conditions read

$$\begin{aligned}
&T_{\mathrm{Ⅱ}}(r_1)=T_{\mathrm{I}}(r_1),\\
&T_{\mathrm{Ⅱ}}(r_2)=T_{\mathrm{Ⅲ}}(r_2),\\
&\kappa_{\mathrm{c}}\frac{\partial T_{\mathrm{Ⅱ}}}{\partial \rho}\Big|_{\rho=r_1}=\kappa_{\mathrm{o}}\frac{\partial T_I}{\partial \rho}\Big|_{\rho=r_1},\\
&\kappa_{\mathrm{c}}\frac{\partial T_{\mathrm{Ⅱ}}}{\partial \rho}\Big|_{\rho=r_2}=\kappa_{\mathrm{b}}\frac{\partial T_{\mathrm{Ⅲ}}}{\partial \rho}\Big|_{\rho=r_2},
\end{aligned} \tag{7}$$

where κ_{o}, κ_{c} and κ_{b} denote the thermal conductivities of object, cloak and background, respectively.

In our method, the parameters κ_{b}, κ_{o}, r_1, and r_2 are fixed, while the inhomogeneity coefficient α can be chosen as the design parameter. When Eq. (7) is satisfied, all cloaks with different α will realize a cloaking effect, but the temperature gradient in the object will change with α. The thermal profile of object can then be manipulated by selecting cloaks with a different inhomogeneity coefficient α. In the specific case of $\alpha=0$, Eq. (7) results in the following relations between the thermal conductivities of different zones:

$$\frac{(\kappa_{\mathrm{c}}+\kappa_{\mathrm{b}})(\kappa_{\mathrm{c}}-\kappa_{\mathrm{o}})}{(\kappa_{\mathrm{c}}-\kappa_{\mathrm{b}})(\kappa_{\mathrm{c}}+\kappa_{\mathrm{o}})}=\frac{r_2^2}{r_1^2}, \tag{8}$$

which is the result of the conventional scattering canceling theory.[27]

Equation (7) cannot be solved analytically. Once a value of α is set, however, the thermal conductivity magnitude of cloak β and the relative thermal gradient of object a_1/a_3 can be calculated numerically.

To verify the above method, a square background (150 mm×150 mm) is considered, where an object (a hole with diameter 50 mm) is embedded in the center of the background. The thermal conductivity of the background, κ_{b}, is 80 $\mathrm{W\cdot m^{-1}K^{-1}}$. The temperatures of the left and right boundaries are 328 K and 278 K, respectively, and the top and bottom boundaries are adiabatic. To cloak the hole ($\kappa=0$) in the center, three different thermal cloaks, where $\alpha=0$, 1, and -1 respectively, are designed. The inner and outer diameters of the cloaks all measure 50 mm and 100 mm, respectively. By solving Eq. (7), we obtain the thermal conductivities of three cloaks as $\kappa_{\mathrm{c}}=133\ \mathrm{W\cdot m^{-1}K^{-1}}$, $89(\rho/r_1)\ \mathrm{W\cdot m^{-1}K^{-1}}$, and $195(\rho/r_1)^{-1}\ \mathrm{W\cdot m^{-1}K^{-1}}$, respectively.

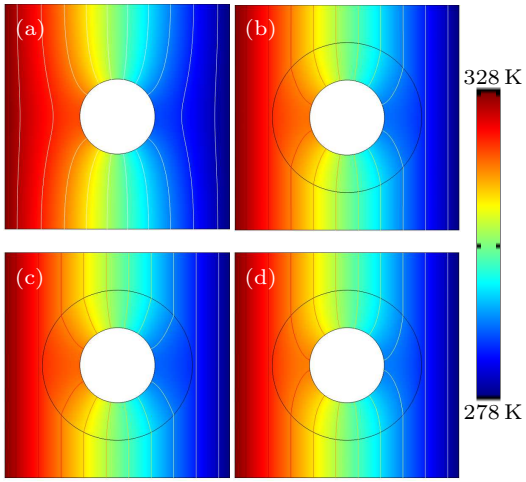

Fig. 2. Temperature profiles caused by a circular hole covered by cloaks with different inhomogeneity: (a) no cloak, (b) cloak with $\alpha = 0$, (c) cloak with $\alpha = 1$, and (d) cloak with $\alpha = -1$.

Table 1. Effective thermal conductivity and diameter of holes in each layer of the cloaks.

Cloak case		Layer				
		1	2	3	4	5
$\alpha = 0$	$\kappa_{\rm eff}$ ($\rm W{\cdot}m^{-1}K^{-1}$)	133	133	133	133	133
	$d_{\rm hole}$ (cm)	0.25	0.25	0.25	0.25	0.25
$\alpha = 1$	$\kappa_{\rm eff}$ ($\rm W{\cdot}m^{-1}K^{-1}$)	98.0	115	133	151	169
	$d_{\rm hole}$ (cm)	0.33	0.29	0.25	0.21	0.17
$\alpha = -1$	$\kappa_{\rm eff}$ ($\rm W{\cdot}m^{-1}K^{-1}$)	177	150	130	115	103
	$d_{\rm hole}$ (cm)	0.14	0.21	0.26	0.29	0.32

The simulated results are shown in Fig. 2. When the hole is not covered by cloak [Fig. 2(a)], this results in curved isothermal lines on the background. When it is covered by the cloaks designed as discussed above [Figs. 2(b)–2(d)], the isothermal lines in the background remain straight, indicating that all the different cloaks can indeed realize a cloaking effect.

Experiments are also carried out for further validation. For practical realization, all cloaks are discrete to five layers, with each layer being 5 mm wide. In each layer, thermal conductivity is homogeneous and isotropic, and is the value at the center of the layer, as shown in Table 1.

To achieve the desired thermal conductivities in different zones, an engineered composite method is applied. A 1-mm-thick alumina plane ($\kappa_{\rm Al} = 200\,\rm W{\cdot}m^{-1}K^{-1}$) is selected as the base material for all the samples. By drilling holes with different diameters on the plane at regular intervals, we can change the effective thermal conductivity of the composite composed by alumina and holes (as shown in the inset of Fig. 3). The effective thermal conductivity of the composite can be calculated based on simulations for heat conduction in a unit cell, and its dependence on the relative diameter of the hole is shown in Fig. 3. As the relative diameter of the hole, d/w, increases, the effective thermal conductivity of the composite, $\kappa_{\rm eff}$, decreases. Based on this result, the diameters of the holes in each layer of the cloak can be determined; these are also listed in Table 1. In the background zone, the diameter of the holes is 3.7 mm. For all structures, the width of the square unit cell is 5 mm.

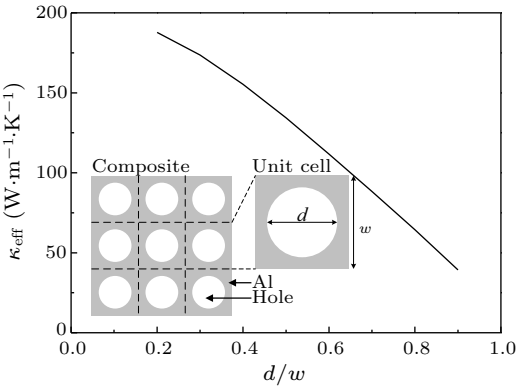

Fig. 3. Effective thermal conductivity of the aluminum composite, varying with the hole diameter. The structure of the composite is shown in the inset.

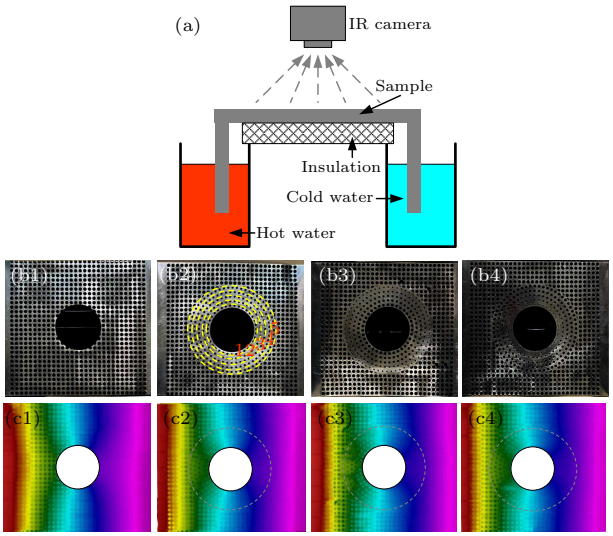

Fig. 4. (a) Experimental schematic. (b1) Photograph of the sample without cloak, and (b2)–(b4) photographs of the samples with cloak for $\alpha = 0$, 1 and -1, respectively. (c1)–(c4) Measured thermal profiles of the samples in (b1)–(b4). The dashed lines indicate the boundary of the cloaks.

The experimental schematic is shown in Fig. 4. The left and right sides of the samples contact with a hot thermostat and a cold thermostat, respectively. When the temperature profiles of the samples stabilize, they are recorded by an infrared camera. The sample photographs and the measured temperature profiles are also shown in Fig. 4. These measured results have the same characteristics as the simulated results shown in Fig. 2, indicating that the cloaks designed by our method do indeed realize a cloaking effect in our experiments.

In the above experiment, the thermal cloaks are designed to cloak a specific object, i.e., a hole where $\kappa = 0$. For objects with finite thermal conductivities, the same method can also be used to design thermal cloaks. In this case, in contrast to the conventional scattering canceling theory based on homogeneous cloaks, our method provides an external freedom, i.e., the inhomogeneity coefficient α, to manipulate the temperature distribution of objects. In this way, in addition to cloaking objects from background, these cloaks can realize additional functions.

For example, consider a circular object with radius $r_1 = 1\,\mathrm{m}$, embedded in the center of a square background with a 6 m edge length. The thermal conductivities of the background and the object are $\kappa_\mathrm{b} = 1\,\mathrm{W{\cdot}m^{-1}K^{-1}}$ and $\kappa_\mathrm{o} = 0.1\,\mathrm{W{\cdot}m^{-1}K^{-1}}$, respectively. The left side and the right side of the background are 400 K and 300 K, while the top and bottom sides are adiabatic. Three different cloaks with the same radius, $r_2 = 2\,\mathrm{m}$, but different α values are designed, based on Eq. (7). With respect to cloak 1, the inhomogeneity coefficient $\alpha = 2$, and the thermal conductivity of the cloak is $\kappa_\mathrm{c} = 0.67(\rho/r_1)^2\,\mathrm{W{\cdot}m^{-1}K^{-1}}$. For cloak 2, $\alpha = -4.4$, and the thermal conductivity of the cloak is $\kappa_\mathrm{c} = 8(\rho/r_1)^{-4.4}\,\mathrm{W{\cdot}m^{-1}K^{-1}}$. For cloak 3, $\alpha = -6$, and the thermal conductivity of the cloak is $\kappa_\mathrm{c} = 15.3(\rho/r_1)^{-6}\,\mathrm{W{\cdot}m^{-1}K^{-1}}$.

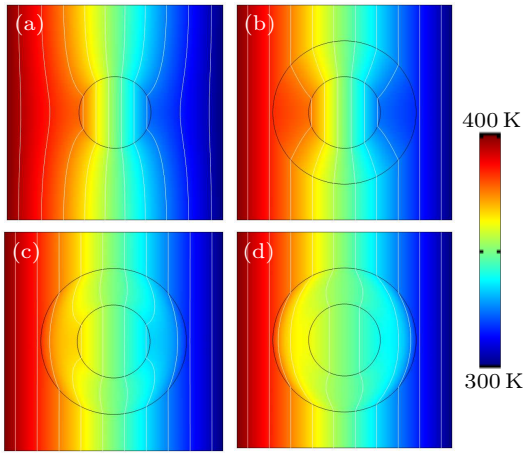

Fig. 5. Simulated temperature profiles for different cases: (a) no cloak, (b) cloak as heat concentrator, (c) cloak for thermal transparency, and (d) cloak for heat shield effect.

The simulated temperature profiles for all the cases are shown in Fig. 5. In Fig. 5(a), the object is not covered by any cloaks, disturbing the temperature profile and resulting in curved isothermal lines on the background. When the object is covered by cloaks [Figs. 5(b)–5(d)], the isothermal lines in the background zone are straight. For cloak 1 [Fig. 5(b)], the thermal gradient in the object is larger than that of the background, indicating that a heat concentration effect is achieved in the object. For cloak 2 [Fig. 5(c)], the thermal gradient in the object is almost the same as that of the background, which realizes the thermal transparency effect. For cloak 3 [Fig. 5(d)], the thermal gradient in the object is smaller than that of the background, which realizes the thermal shield effect for the object.

The temperature profiles along the x-axis for each different case are shown in Fig. 6, to provide a more detailed for comparison. When the object is covered by cloaks, the temperature profiles are the same as those of the reference line (uniform background without object embedded) in the background zone, indicating that all cloaks provide a good cloaking effect. The object, however, has different temperature gradients, i.e., 1.63, 1.0, and 0.72 times of that of the background, respectively. These results verify our proposal that the thermal profiles of objects can be manipulated by means of the inhomogeneity of the cloaks with isotropic thermal conductivity. Huang *et al.*[25] provided another framework to realize this manipulation based on multilayer anisotropic materials or gradient anisotropic materials. In contrast to their work, only isotropic materials are required in our method. This characteristic may make the cloaks more practical in engineering terms, given their employment of natural materials. In this work, circular objects and annular cloaks are applied and designed for simplicity. The same method may be applied to objects with other shapes, such as elliptical objects. Han *et al.*[28] have designed elliptical thermal cloaks based on isotropic and homogenous materials. As an additional design factor, the inhomogeneity of the elliptical cloaks should also work as it does for the circular counterpart.

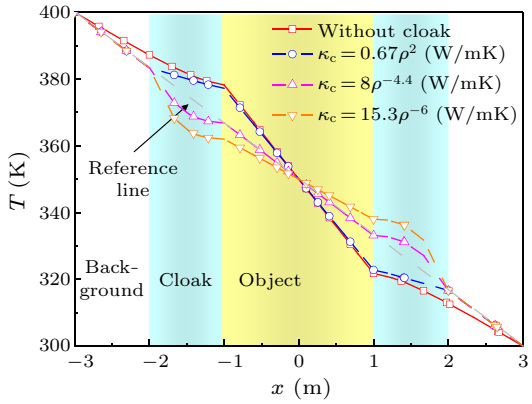

Fig. 6. Temperature distributions along the x axis.

The thermal gradient of the object depends not only on the inhomogeneity of the cloak, but also on other parameters, such as the thermal conductivity of the object, and the relative scale of the cloak. Figure 7(a) shows the variation of the thermal gradient of object a_1 (normalized by the thermal gradient of back-

ground a_3) for different object thermal conductivities. The relative scale of the cloak is fixed ($r_2/r_1 = 2$). In all these cases, the relative thermal gradient of object a_1/a_3 can only vary from 0 to a finite value. When the cloak has very large inhomogeneity ($\alpha \to \pm\infty$), the thermal gradient of the object decreases to zero. When α is very large, there must be very low thermal conductivity in some areas of the cloak. In this way, the heat flux from background can barely go through the cloak, such that no thermal gradient can be established on the object covered by the cloak. As the thermal conductivity of the object increases, the range of a_1/a_3 narrows down. When $\kappa_o/\kappa_b < 1$, the maximum of a_1/a_3 will be greater than 1. As $\kappa_o/\kappa_b = 1$, the maximum of a_1/a_3 is 1. As $\kappa_o/\kappa_b > 1$, the maximum of a_1/a_3 will be less than 1. This can be easily understood in relation to the fact that high thermal conductivity will lead to a low thermal gradient for a constant heat flux.

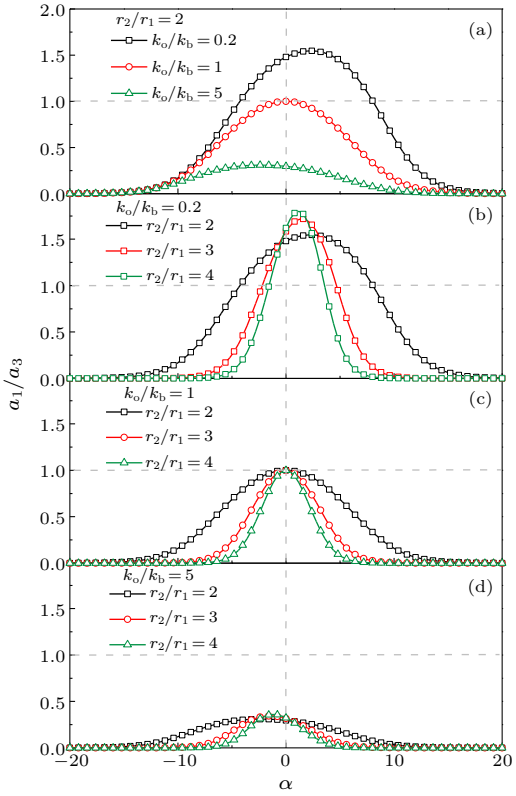

Fig. 7. Normalized thermal gradient of object a_1/a_3, varying for different cases.

The effects of the cloak scale on the adjustable range of the thermal gradient of an object are also studied. Figures 7(b)–7(d) show the variation of a_1/a_3 for different cloak scales with an object with fixed thermal conductivity, i.e., $\kappa_o/\kappa_b = 0.2$, 1, and 5, respectively. For the case of $\kappa_o/\kappa_b > 1$ or $\kappa_o/\kappa_b < 1$, the adjustable range of a_1/a_3 will increase slowly with an increase in cloak thickness, demonstrating that thick cloaks have a greater capacity for thermal manipulation. However, no matter how large the cloak is, there must be a limitation for a_1/a_3. This is shown clearly in the specific case of $\kappa_o/\kappa_b = 1$ [Fig. 7(c)], where the maximum of a_1/a_3 is always 1, independent of the scale of the cloak. When κ_o/κ_b is fixed, the maximum of a_1/a_3 is almost the same as the value in the case without a cloak. This is illustrated in Figs. 6 and 7(c). In Fig. 6, the magnitudes of thermal gradient for an object covered by different cloaks are always lower than for an object without a cloak. In Fig. 7(c), a_1/a_3 should clearly be 1, when the object (not covered by cloaks) has the same thermal conductivity as the background. Although increasing the thickness of cloaks will not increase the adjustable range of the object's thermal gradient, it will help to decrease the inhomogeneity of the cloaks for a fixed thermal gradient of object, rendering the cloak more realizable. Therefore, a tradeoff should be made between the scale of the cloak and the inhomogeneity of the cloak in terms of practical design.

In summary, we have proposed a new method, based solely on isotropic materials for the design of thermal cloaks in a steady heat conduction regime. The thermal conductivity of the cloak designed by our method varies exponentially with radius. When objects are covered by the cloak, they will not disturb the temperature profile in the background zone. In addition, the external design freedom, i.e., the inhomogeneity of the cloak, can help to manipulate the temperature profile of the objects. Therefore, thermal transparency, heat concentration, or thermal shield effects can all be realized in a unified framework. Our method is validated by simulations and experiments. Given their isotropic properties, these cloaks may be easily fabricated. The same method can be applied to design other cloaks, such as electrical, magnetic, or acoustic cloaks.

References

[1] Fan C Z, Gao Y and Huang J P 2008 *Appl. Phys. Lett.* **92** 251907
[2] Yang T Z, Huang L J, Chen F and Xu W K 2013 *J. Phys. D* **46** 305102
[3] Dede E M, Nomura T, Schmalenberg P and Lee J S 2013 *Appl. Phys. Lett.* **103** 63501
[4] Guenneau S, Amra C and Veynante D 2012 *Opt. Express* **20** 8207
[5] Ye Z Q and Cao B Y 2016 *Phys. Chem. Chem. Phys.* **18** 32952
[6] Chen F and Lei D Y 2015 *Sci. Rep.* **5** 11552
[7] Hu R, Wei X, Hu J and Luo X 2014 *Sci. Rep.* **4** 3600
[8] Narayana S, Savo S and Sato Y 2013 *Appl. Phys. Lett.* **102** 201904
[9] Guenneau S and Amra C 2013 *Opt. Express* **21** 6578
[10] Vemuri K P, Canbazoglu F M and Bandaru P R 2014 *Appl. Phys. Lett.* **105** 193904
[11] Liu Y, Jiang W, He S and Ma Y 2014 *Opt. Express* **22** 17006

[12] Li Y, Shen X, Wu Z, Huang J, Chen Y, Ni Y and Huang J 2015 *Phys. Rev. Lett.* **115** 195503
[13] Hu R, Zhou S, Li Y, Lei D, Luo X and Qiu C 2018 *Adv. Mater.* **30** 1707237
[14] Hou Q, Zhao X, Meng T and Liu C 2016 *Appl. Phys. Lett.* **109** 103506
[15] Sun F and He S 2017 *Sci. Rep.* **7** 40949
[16] Hu R, Huang S, Wang M, Luo X, Shiomi J and Qiu C W 2019 *Adv. Mater.* **31** 1807849
[17] Kang S, Cha J, Seo K, Kim S, Cha Y, Lee H, Park J and Choi W 2019 *Int. J. Heat Mass Transfer* **130** 469
[18] Han T C, Yuan T, Li B W and Qiu C W 2013 *Sci. Rep.* **3** 1593
[19] Hou Q, Yin J, Zhao X and Bi Y 2018 *Phys. Lett. A* **382** 2382
[20] Han T, Bai X, Gao D, Thong J T L, Li B and Qiu C 2014 *Phys. Rev. Lett.* **112** 54302
[21] Xu H, Shi X, Gao F, Sun H and Zhang B 2014 *Phys. Rev. Lett.* **112** 54301
[22] Yang T, Bai X, Gao D, Wu L, Li B, Thong J T L and Qiu C 2015 *Adv. Mater.* **27** 7752
[23] Xu G, Zhang H, Xie M and Jin Y 2017 *AIP Adv.* **7** 105322
[24] Hu R, Huang S, Wang M, Zhou L, Peng X and Luo X 2018 *Phys. Rev. Appl.* **10** 054032
[25] Wang R, Xu L, Ji Q and Huang J 2018 *J. Appl. Phys.* **123** 115117
[26] Narayana S and Sato Y 2012 *Phys. Rev. Lett.* **108** 214303
[27] He X and Wu L 2013 *Phys. Rev. E* **88** 33201
[28] Han T, Yang P, Li Y, Lei D, Li B, Hippalgaonkar K and Qiu C 2018 *Adv. Mater.* **30** 1804019